
Darrel M. Kingfield

The effect of urban environments on storm evolution through a radar-based climatology of the central United States

Darrel M. Kingfield[1,2,3], Kristin M. Calhoun[1,2], Kirsten de Beurs[3], Geoffrey Henebry[4]
[1]Cooperative Institute for Mesoscale Meteorological Studies, University of Oklahoma, United States of America;
[2]NOAA/OAR/National Severe Storms Laboratory, United States of America;
[3]Dept. of Geography and Environmental Sustainability, University of Oklahoma, United States of America;
[4]Geospatial Sciences Center of Excellence, South Dakota State University, United States of America

Dated: 15 June 2015

1. Introduction

There is an upward trend in urbanization from 30% in 1950 to 54% today with an estimated 66% of the global population living in urban areas by 2050 (UN 2014). In North America, around 82% of the population currently resides in urban areas with an estimated density of impervious surface area for the conterminous United States (CONUS) of around 112,610 km^2 (Elvidge et al. 2004). Hypotheses on precipitation modification by major urban areas have been around for quite some time (e.g. Horton 1921; Landsberg 1956; Shepherd 2005) with many climatological studies showing precipitation enhancement particularly downwind of major cities and altered storm composition (e.g. Changnon et al. 1981; Shepherd et al. 2002; Niyogi et al. 2011), however, studies on the influences of small to mid-size cites have received less attention.

This study examines the role of the urban environment on the spatiotemporal characteristics of supercells through a multi-year, multi-radar climatology of Weather Service Radar – 1988 Doppler (WSR-88D) radar reflectivity and algorithmic variables from 2009 to 2013 for four cities in the United States Central Plains: Minneapolis, MN, Omaha, NE, Oklahoma City, OK, and Dallas-Fort Worth, TX. These initial five years were chosen as they represent a uniform series of "super-resolution" (Torres and Curtis 2007) reflectivity and velocity data. Super-resolution enhances the quality of base radar variables by reducing the effective scanning beamwidth from 1.38° to 1.02° and allowing for vortex and other storm-scale features to be resolved at longer ranges from any single WSR-88D (Brown et al. 2002; Brown et al. 2005). The Central Plains were chosen as this region experiences frequent severe weather events and contains urban regions with a diverse range of shapes, sizes, and populations.

2. Data & Methods

2.1 Case & Radar Identification

Event days with supercell morphologies were chosen by utilizing the significant severe events database (Smith et al. 2012) which provides the largest manual analysis of convective modes over the CONUS to date. Candidate cases were chosen beginning with any significant severe weather event occurring within a 200km^2 domain around each of the four cities. For each case date of interest, a processing window of +/- one convective day (~24 hours) around the event was also processed to ensure the storms of interest and any subsequent ancillary convection around the main event were retained. All WSR-88D radars within 300km of each city domain had their raw data downloaded from the National Centers for Environmental Information (NCEI) for reprocessing. In total, data from 56 (36 unique) WSR-88Ds and 1,604,446 convective volume scans across 808 days were processed (Table 1).

City/Domain	Number of WSR-88D Radars	Number of Case Dates Processed
Minneapolis, MN, USA	12	158
Omaha, NE, USA	12	186
Oklahoma City, OK, USA	15	245
Dallas-Fort Worth, TX, USA	17	219

Table 1: Total number of radars and cases processed for each city domain.

2.2 Quality Control & Data Processing

The Warning Decision Support System – Integrated Information (WDSS-II; Lakshmanan et al. 2007b) system was used to ingest, quality control, generate multi-radar fields, and track all storms in the study. First, radar reflectivity data were quality controlled through a neural network framework to remove non-meteorological scatterers (e.g. biological targets, clutter, test/interference patterns) while retaining precipitation returns (Lakshmanan et al. 2007a). Velocity data were quality controlled utilizing a two-dimensional velocity dealiasing framework (Jing and Wiener 1993) with model-derived vertical sounding products from the Rapid Update Cycle/Rapid Refresh (Benjamin et al. 2004) to enhance the quality of the input radial velocity fields (Miller et al.

2013).

These quality controlled polar coordinate base fields served as inputs into an intelligent agent framework (Lakshmanan et al. 2006) to generate a Cartesian multi-radar grid of base and derivative products with at least 1km spatial resolution, one min. temporal resolution, and 33 vertical levels. This "cube" of radar and algorithmic outputs served as the inputs following the methodology of Lakshmanan and Smith (2009) to identify and attach environmental attributes to storm clusters. All storms were identified and tracked twice for this study. Initially, storms were identified using composite reflectivity to automatically classify supercell convective modes by following the methodology of Hobson et al. (2012). Following the storm type classification tracking, these clusters were tracked again at the -10°C isothermal level to better assess storm size and aspect ratio for attribute attachment. For both iterations, a combination of watershed segmentation and k-means clustering were used to identify the storm objects (Lakshmanan et al. 2009). To complete the storm identification, the algorithm searches for local maxima in reflectivity greater than 20 dBZ, then incrementally grows the area until it is at least 200 km^2. A storm cluster is then matched with a separately identified cluster at the next time step (for our analysis, a one min. time step was used) using a cost function, where longer-lived cells are given preference in the case of storm mergers. In addition to radar and lightning characteristics being monitored at each time step, storm position with reference to the urban boundaries of each city was also tracked.

At the end of the second storm-tracking step, path segments were assembled by connecting the centroid positions between each subsequent minute for the lifetime of the tracked storm. At this juncture, storm trajectories classified as supercells were retained while non-supercell structures were discarded. All subsequent supercell tracks were split into two groups as to whether or not they crossed the urban boundary. For storms that did interact with the urban boundary, storm lifetime before, during, and after the city were calculated. For all supercell trajectories, storm attributes from each tracked storm cluster were sampled every 10 min., noting the longest decorrelation times were around 9 min. from a similar study (Herzog et al. 2014). The decorrelation time can be found by determining the lag at which the autocorrelation function falls below 1/*e* for each attribute (Rudlosky and Fuelberg 2013).

2.3 Grid Accumulations Independent of Convective Mode

To accompany the attribute extraction for supercells, grids of composite reflectivity, Maximum Expected Size of Hail (MESH) (Witt et al. 1998), and cloud-to-ground (CG) lightning density data from the US National Lightning Detection Network (NLDN) (Orville, 1998) independent of convective mode were accumulated daily. In each of the three accumulated grids, the maximum value for each grid point is retained so instances of training events (i.e. repeated areas of precipitation over a single location) are not counted multiple times. For composite reflectivity, the number of days exceeding 40 dBZ was accumulated in each study domain. This threshold has been used in prior studies to discriminate between convective and stratiform regimes (e.g. Falconer 1984; Rickenback & Rutledge 1998; Parker and Knievel 2005; Bentley et al. 2010). For MESH, the number of days per pixel exhibiting non-severe (21mm <= MESH < 29mm) and severe estimated hail sizes (MESH >= 29mm) were accumulated. These intensity thresholds were determined in Cintineo et al. (2012) to have the best discrimination skill to observed hail on the ground. To mitigate spurious noise while retaining valid storm tracks, the MESH grids went through three stages of dilation (90th percentile) and erosion (25th percentile). For NLDN lightning density, each pixel was accumulated when the maximum lightning density (in $min^{-1}km^2$) exceeded 0.1 as an experimental threshold.

3. Results

3.1 Frequency of Observations and Supercell Lifetime

The frequency and lifetime of supercell objects identified through the above tracking varied by geography and interaction with the city (Table 2). As expected, the number of supercells interacting with each urban domain was positively correlated to urban size. In all four city domains, supercells interacting with the urban domain had a longer mean lifetime when compared to supercells outside the urban domain. In both Minneapolis and Oklahoma City, the differences in the means were statistically significant at the 99% confidence interval through a two-sample non-parametric permutation test (Wilks 2011).

City/Domain	Non-City Supercell Lifetime	City Supercell Lifetime	p-value
Minneapolis, MN, USA	72.09 min. (N=953)	87.80 min. (N=234)	<0.001
Omaha, NE, USA	74.76 min. (N=1528)	75.19 min. (N=207)	0.92
Oklahoma City, OK, USA	87.25 min. (N=1917)	121.17 min. (N=252)	<0.001
Dallas-Fort Worth, TX, USA	90.82 min. (N=1647)	95.14 min. (N=436)	0.30

Table 2: Mean supercell lifetime for storms interacting and not interacting with the city domain and results of a two-sample non-parametric permutation test of the mean.

3.2 Trends in Radar-Derived Supercell Attributes

Evaluating the MESH distributions (Fig. 1) for supercells, there is a substantial amount of overlap between the distributions when comparing city and non-city storms. For supercells that interact with the urban environment, the median MESH values are the strongest before entering the urban domain and subsequently weaken during and after urban interaction. The exception to this is Omaha; Omaha had an increase in median MESH for observations after urban interaction, however, the comparison between the medians are not statistically significant at the 95% confidence interval. Supercells that do not interact with the urban domain at all have a similar spread in the distribution with a higher median than supercells entering and departing the urban domain.

In an attempt to isolate only the "mature" portion of the supercell and remove observations in the growth and decay stages, a variable time window from 0 to 30 min. in five min. intervals were used on both sides of the supercell lifecycle. Adding more time before the first sample in the lifecycle does slightly increase both the pre-city/no-city observations but does little to separate the observations overall. Similar trends were observed when limiting the final observation in the supercell lifecycle.

Similar results in terms of distribution overlap were observed when evaluating composite reflectivity (Fig. 2). For Minneapolis, Omaha, and Dallas-Fort Worth, non-statistically significant increases in median composite reflectivity were observed from the samples over the urban domain compared to pre-urban interaction. In Oklahoma City, the median composite reflectivity is the highest before the city and declines during/post-urban interaction. In all four domains, the median reflectivity in the post-urban observations is the lowest for all supercell distributions. In all domains except Omaha, this lower median is statistically significant at the 95% confidence interval when compared to the medians of pre-urban, urban, and non-urban distributions.

3.3 Time Accumulated Grids of Radar & Derivative Products

For domains other than Minneapolis, gridded accumulations of lightning density (Fig. 3) show an elevated number of days with a CG density greater than 0.1 $min^{-1}km^{2}$ within the urban domain. For Oklahoma and Dallas-Fort Worth, regions downstream from the urban domain to the east and northeast respectively show equivalent density counts. In Omaha, elevated density counts are observed in the southeast part of the study domain with counts comparable to levels observed within the urban domain. In the Minneapolis area, lightning counts are the lowest with fewer than nine days observed in most parts of the domain.

Gridded accumulations of severe MESH (Fig. 4) and non-severe MESH also show no preferred alignment and position to the urban domain with regions of equivalent counts occurring both in and around the urban domain, particularly upstream. With generally higher values of MESH upstream of the urban domain (Fig. 1), it is anticipated that higher daily counts would be observed on the maps in those locations (Fig. 4). Several non-urban supercells also contribute to these counts with several tracks observed to the north of the Dallas-Fort Worth domain, north and south of the Oklahoma City domain, and south of the Omaha domain. Similar in behavior to the CG density plots, the Minneapolis domain showed the fewest number of severe hail days with an almost random pattern of swaths across the study domain.

4. Discussion

Radar-derived, automated climatologies provide an efficient and ubiquitous mechanism to study a large sample of storms without the labor-intensive process of manual categorization; however, leaving this process to automation can introduce errors. The nature by which a storm fills a radar beam is highly variable with range/height considerations that can yield multiple solutions from different radars at a single time step. Furthermore, with radar reflectivity determined by particle diameter, even a small amount of larger particles in a volume can enhance returns and provide an inflated severity. This is especially the case when the beam is diverted and filled with non-meteorological objects (e.g. wind turbines). While non-meteorological contamination can easily be rectified by a manual observer through indigenous knowledge of a region, an automated system may retain these signatures, leaving radial spikes and other artifacts in the climatology. With 1,604,446 convective volume scans in this automated analysis, there is the strong possibility that artifacts do remain.

In evaluating all of the data, there is a general decaying trend for supercell storms after interacting with the urban domain, however, a more intensive lifetime analysis needs to be undertaken. How "old" are these storms before urban interaction? By evaluating the location of convective initiation, some signal may be parsed out as to where storms are forming spatially compared to these cities. Furthermore, evaluating only "younger" storms that interact with the urban domain may yield a more unique trend compared to non-city interacting supercells.

5. Summary

This study is the culmination of a five-year multi-radar/multi-sensor attribute tracking analysis of 7,174 supercell storms in and around four urban domains in the Central Plains. When evaluating all of these data together, mean supercell lifetimes were longer for storms interacting with the urban domain compared supercells that missed this domain. Tracking radar-derived supercell attributes through their lifetime, a general decaying trend is observed in

these variables during and after interaction with the urban domain for most combinations of variables and domains. When compared to non-urban supercells, distributions of MESH, composite reflectivity, and other radar variables show a large amount of overlap in the ranges of values observed. The positions of radar and lightning-derived peaks on count maps exceeding certain thresholds also showed no preferred bullseye over the city with similar counts observed both upstream and downstream of the urban domain. Expansion of the dataset to include additional years, convective initiation points, and additional permutations of variables and lifetime ranges are planned.

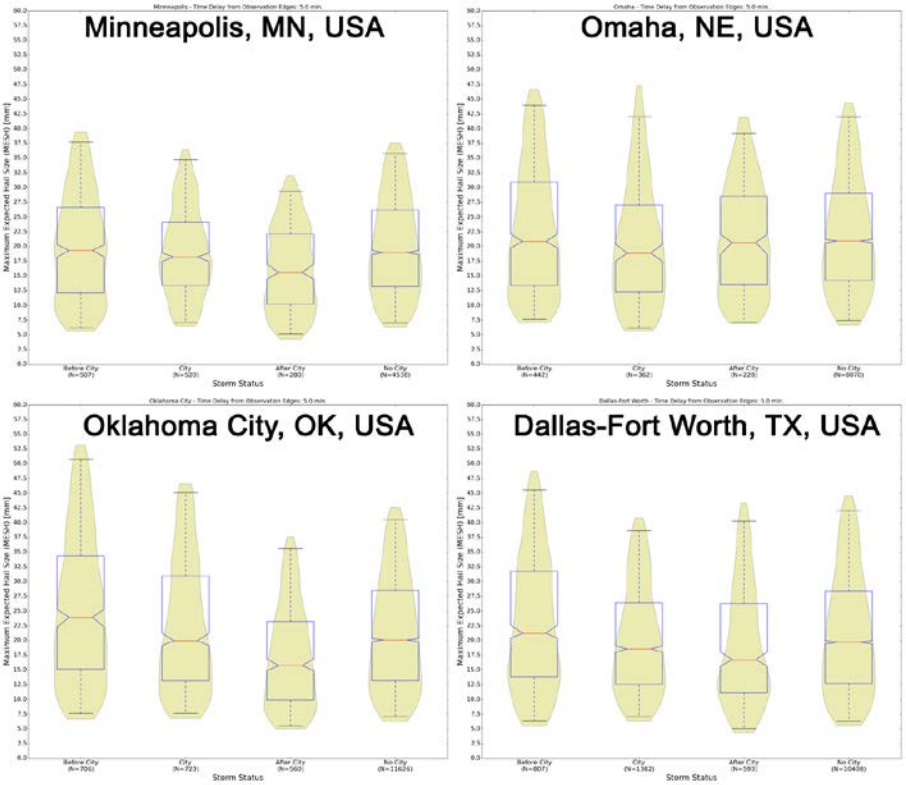

Fig. 1: MESH values extracted every 10 min. for supercells before, during, and after interaction with the urban domain as well as supercells with no interaction with the urban domain.

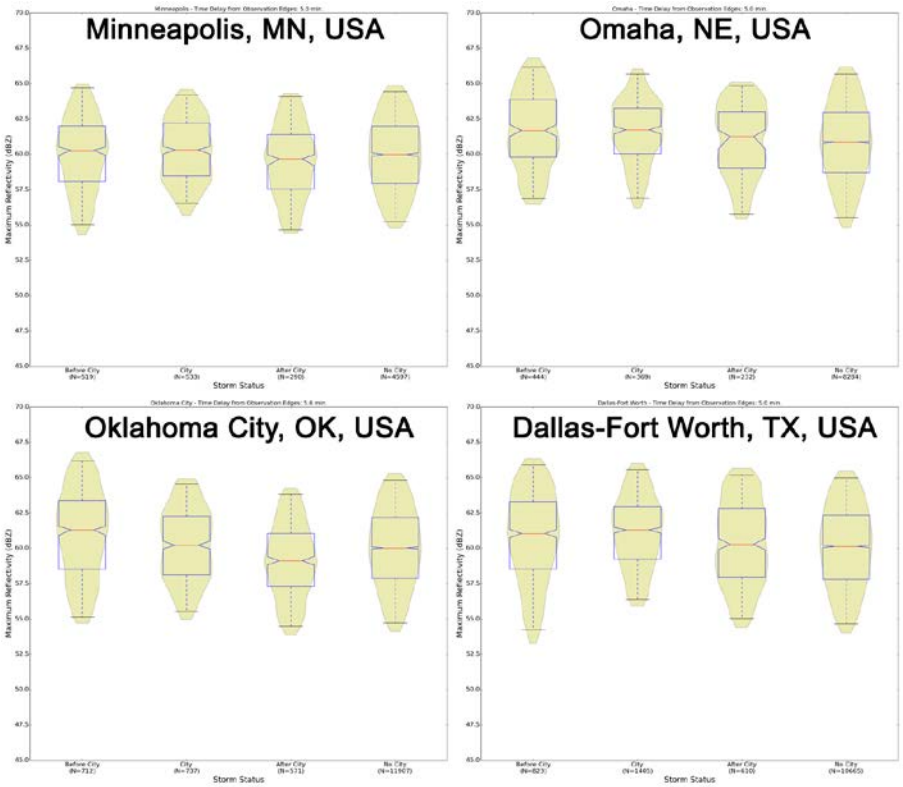

Fig. 2: Composite reflectivity values extracted every 10 min. for supercells before, during, and after interaction with the urban domain as well as supercells with no interaction with the urban domain.

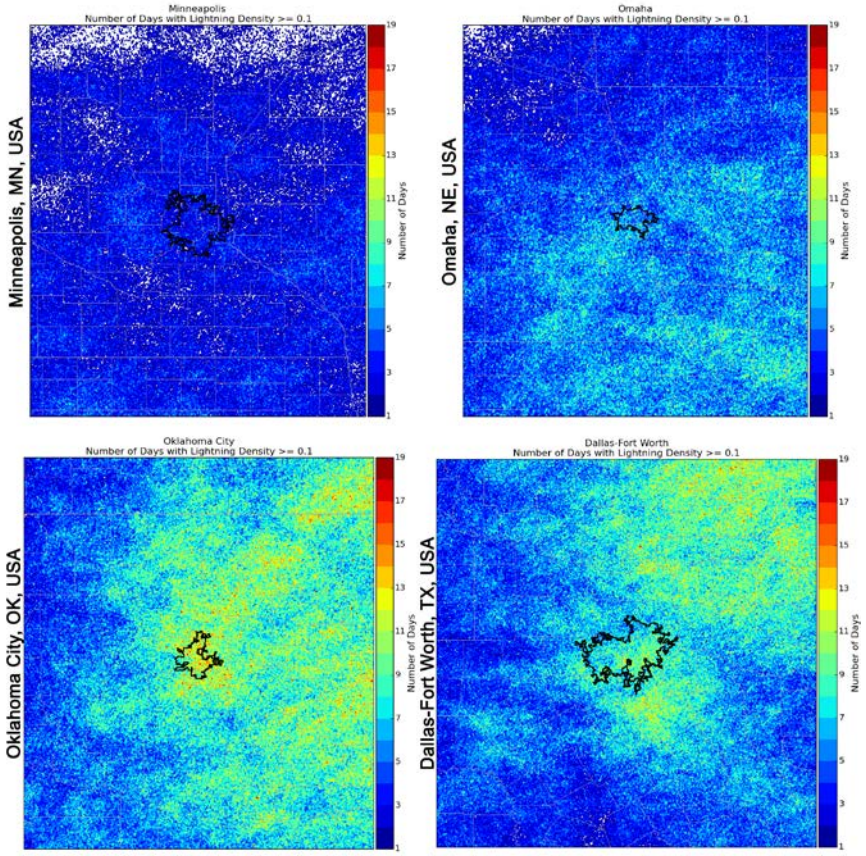

Fig. 3: Number of days with a gridded CG lightning density greater than 0.10 $min^{-1}km^{2}$. The urban domain is outlined in black in the center of each map.

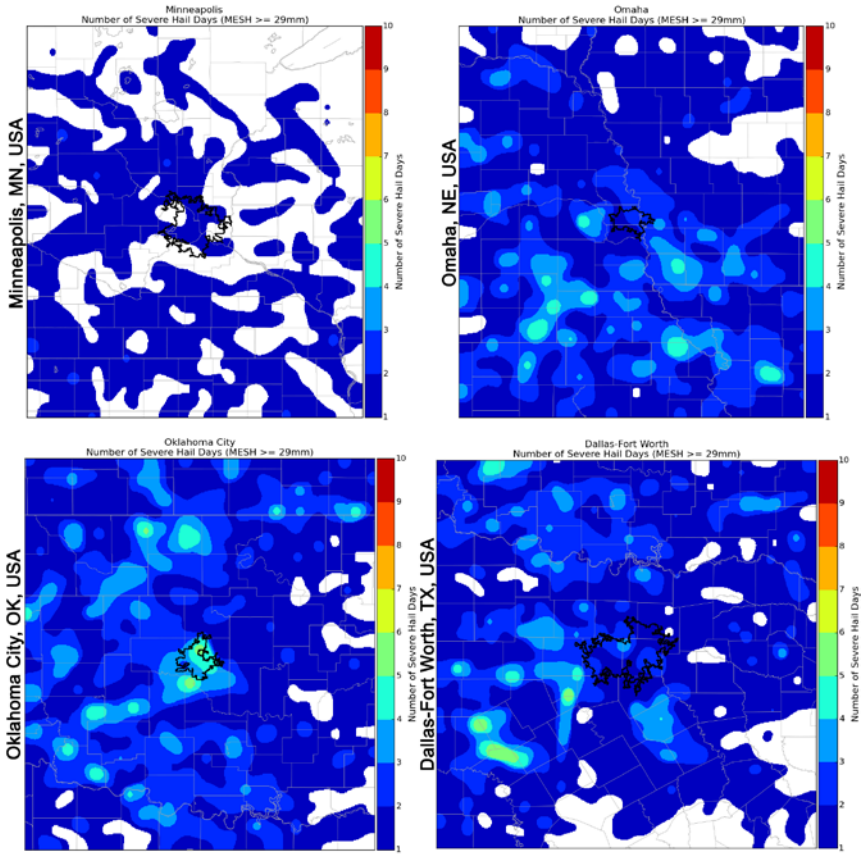

Fig. 4: Number of days with MESH exceeding the severe hail criterion of 29mm. The urban domain is outlined in black in the center of each map.

Acknowledgments

This work is funded through the NASA Interdisciplinary Science Program project NNX12AM89G as part of the grant “Storms, Forms, and Complexity of the Urban Canopy: How Land Use, Settlement Patterns, and the Shapes of Cities Influence Severe Weather.”

References

Benjamin, S. G., and Coauthors, 2004: An hourly assimilation-forecast cycle: The RUC. *Mon. Wea. Rev.*, **132**, 495-518.

Brown, R. A., V. T. Wood, and D. Sirmans, 2002: Improved tornado detection using simulated and actual WSR-88D data with enhanced resolution. *J. Atmos. Oceanic Technol.,* **19**, 1759-1771.

_____, and Coauthors, 2005: Improved detection of severe storms using experimental fine-resolution WSR-88D measurements. *Wea. Forecasting*, **20**, 3-14.

Changnon, S. A., R. G. Semonin, A. H. Auer, R. R. Braham, and J. Hales, 1981: METROMEX: A Review and Summary. *Meteor. Monogr.,* **40**, Amer. Meteor. Soc., 81pp.

Cintineo, J. L., T. M. Smith, V. Lakshmanan, H. E. Brooks, and K. L. Ortega, 2012: An objective high-resolution hail climatology for the contiguous United States. *Wea. Forecasting*, **27**, 1235-1248.

Elvidge, C. D., and Coauthors, 2004: U.S. constructed area approaches the size of Ohio. *Eos. Trans. Amer. Geophys. Union*, **85**, 233.

Falconer, P. D., 1984: A radar-based climatology of thunderstorm days across New York state. *J. Climate Appl. Meteor.*, **23**, 1115-1120.

Herzog, B. S., K. M. Calhoun, and D. R. MacGorman, 2014: Total lightning information in a 5-year thunderstorm climatology. *XV International Conference on Atmospheric Electricity*. 21pp.

Hobson, A. G., V. Lakshmanan, T. M. Smith, and M. Richman, 2012: An automated technique to categorize storm type from radar and near-storm environment data. *Atmos. Res.*, **111**, 104-113.

Horton, R. E., 1921: Thunderstorm breeding spots. *Mon. Wea. Rev.*, **49**, 193-194.

Jing, Z., and G. Wiener, 1993: Two-dimensional dealiasing of Doppler velocities. *J. Atmos. Oceanic Technol.*, **10**, 798-808.

Landsberg, H. E., 1956: The climate of towns. *Man's Role on Change the Face of the Earth*, W. L. Thomas, Ed., Univ. of Chicago Press, 584-606.

Lakshmanan, V., T. Smith, K. Hondl, G. J. Stumpf, and A. Witt, 2006: A real-time, three-dimensional, rapidly updating, heterogeneous radar merger technique for reflectivity, velocity, and derived products. *Wea. Forecasting*, **21**, 802-823.

_____, A. Fritz, T. Smith, K. Hondl and G. Stumpf, 2007a: An automated technique to quality control radar reflectivity data, *J. Appl. Meteor. Climatol.*¸**46**, 288-305.

_____, T. Smith, G. Stumpf, and K. Hondl, 2007b: The warning decision support system – integrated information. *Wea. Forecasting*, **22**, 596-612.

_____, K. Hondl, and R. Rabin, 2009: An efficient, general-purpose technique for identifying storm cells in geospatial images. *J. Ocean. Atmos. Tech.*, **26**, 523-37.

_____, and T. Smith, 2009: Data mining storm attributes from spatial grids. *J. Atmos. Oceanic Technol.*, **26**, 2353-2365.

Miller, M. L., V. Lakshmanan, and T. M. Smith, 2013: An automated method for depicting mesocyclone paths and intensities. *Wea. Forecasting*, **28**, 570-585.

Niyogi, D., and Coauthors, 2011: Urban modification of thunderstorms: An observational storm climatology and model case study for the Indianapolis urban region. *J. Appl. Meteor. Climatol.*,**50**, 1129-1144.

Orville, R. E., 1998: Development of the National Lightning Detection Network. *Bull. Amer. Meteor. Soc.*, **89**, 180-190.

Parker, M. D., and J. C. Knievel, 2005: Do meteorologists suppress thunderstorms? Radar-derived statistics and behaviour of moist convection. *Bull. Amer. Meteor. Soc.*¸**86**, 341-358.

Rickenbach, T. M, and S. A. Rutledge, 1998: Convection in TOGA COARE: horizontal scale, morphology, and rainfall production. *J. Atmos. Sci.*, **55**, 2715-2729.

Rudlosky, S. D., and H. E. Fuelberg, 2013: Documenting storm severity in the mid-atlantic region using lightning and radar information. *Mon. Wea. Rev.*, **141**, 3186-3202.

Shepherd, J. M., H. Pierce, and A. J. Negri, 2002: Rainfall modifications by major urban areas: Observations from spaceborne rain radar on the TRMM satellite. *J. Appl. Meteor.*, **41.** 689-701.

_____, 2005: A review of current investigations of urban-induced rainfall and recommendations for the future. *Earth Interact.*, **9**, 1-27.

Smith, B. T., R. L. Thompson, J. S. Grams, and C. Broyles, 2012: Convective modes for significant severe thunderstorms in the contiguous United States, Part I: Storm classification and climatology. *Wea. Forecasting*, **27**, 1114-1135.

Torres, S. M., and C. D. Curtis, 2007: Initial implementation of super-resolution data on the NEXRAD network. Preprints, *23rd Conf. on Information Processing Systems*, San Antonio, TX, Amer. Meteor. Soc. 5B.10.

United Nations, Department of Economic & Social Affairs, Population Division, 2014: World Urbanization Prospects: The 2014 Revision, Highlights. *United Nations*, New York, 32pp.

Wilks, D. S., 2011: Statistical methods in the atmospheric sciences. *Academic Press*, 676pp.

Witt, A., M. D. Eilts, G. S. Stumpf, J. T. Johnson, E. D. Mitchell, and K. W. Thomas, 1998: An enhanced hail detection algorithm for the WSR-88D. *Wea. Forecasting*, **13**, 286-303.